DEM simulation of rock fragmentation and size distribution under different loading conditions

Yucang Wang and Fernando Alonso-Marroquin

ESSCC, the University of Queensland, Brisbane, Australia

Abstract

Rock fracture and fragmentation play importance roles in earthquakes, structural engineering and comminution processes. Typically, the measured size distribution of the fragments is given by power law relations. Those relations are independent on the energy input and the loading conditions. In this study, we use ESyS_Particle, the 3-D parallel Discrete Element Model, to simulate rocks as an assemblage of bonded spherical particles. ESyS_Particle takes into account single particle rotation and full set of interactions between the bonded particles. The model is suitable for brittle rock fracture and fragmentation processes. We reproduce the fracture process and calculate the size distribution of the fragments using two different loading conditions: 1) slow and quasi-static uni-axial compression of rock-like samples; 2) fast loading by throwing a sphere consisting of small bonded particles to a rigid wall. Realistic fracture patterns and fragment size distribution are obtained.

1 Introduction

Quasistatic and dynamic fragmentation is a complex and interesting phenomena observed in geological and industrial processes. Rock attrition is a wearing mechanism of fault gouges during the quasistatic deformation imposed by the tectonic plates. Rock pulverization during earthquakes leads to fine grain gouges, which are thought to control earthquake instabilities (Wilson et al 2005). In the mining industry, understanding rock fragmentation is essential as it provides indications of how efficiently rocks can be broken to separate ore from waste materials (Kanchibotla, 2003).

In mineral processing, an important issue is to determine how the input energy is transformed in surface fracture energy, dissipation and kinetic energy during fragmentation. An essential question is: What is the correlation between the input energy and the size distribution of fragments? Experimental and numerical experiments have been done, such as quasistatic and dynamic compression of balls between two rigid walls (Thornton et al 2004), impact test of spheres against rigid walls (Wu et al 2004), binary collision of disks (Kun et al 1999) and explosion of closed shells (Wittel et al 2004). These investigations lead to a common conclusion: When the input energy is large enough, the distribution of size of the fragments obeys power law relations. In particular, numerical experiments with colliding disks show that wide range of input energy lead to the same size distribution of fragments (Kun et al 1999). On the other hand, experiments

with bulky balls suggest that size distribution is affected with input energy, as more energy produces more fines (Wu ET all 2004).

In laboratory tests, fracture process occurs too fast to be observed in detail. Numerical models, such as Discrete Element Method, do not have this limitation. With the recent advances of large scale simulations, numerical simulations represent an attractive alternative, as they provide detailed information on breaking of bonds and velocity distribution of the fragments that are not easily accessible in experiments. Numerics also allow calculating energy budget during fragmentation in earthquakes, which may provide explanation to the heat flow anomalies observed in fault zones. Some numerical studies using aggregates of bonded particles have been used to understand fragmentation process (Kun et al 1999, Wittel et al 2004, Thornton et al 2004).

As a first step to understand fragmentation phenomenon, we use our Discrete Element software, ESyS_Particle, to model brittle rock fracture under two different loading conditions. We are particularly interested in the fracture patterns and fragment size distribution.

2 ESyS_Particle model

ESyS_Particle, previously called Lattice Solid Model or LSMearth, is the Discrete Element Method (DEM) developed in ESSCC, the University of Queensland. It has been applied to the study of physical process such as rock fracture and earthquakes (Wang et al 2006). There are several important features which distinguish the ESyS_Particle from the other existing DEMs, as we will address briefly below.

2.1 Particle rotation

The first one is explicit representing of particle orientation. The unit quaternion $q = q_0 + q_1 i + q_2 j + q_3 k$ is used to describe the orientations of particles (Wang et al 2006). The physical meaning of a quaternion is that it represents a one-step rotation around the vector $q_1\hat{i} + q_2\hat{j} + q_3\hat{k}$ with a rotation angle of $2\mathbf{arccos}(q_0)$. A quaternion for each particle satisfies the following equation

$$\dot{\boldsymbol{Q}} = \frac{1}{2}\boldsymbol{Q_0}(q)\,\boldsymbol{\Omega}\,, \tag{1}$$

Where $\dot{\boldsymbol{Q}} = \begin{pmatrix} \dot{q}_0 \\ \dot{q}_1 \\ \dot{q}_2 \\ \dot{q}_3 \end{pmatrix}$, $\boldsymbol{Q_0}(q) = \begin{pmatrix} q_0 & -q_1 & -q_2 & -q_3 \\ q_1 & q_0 & -q_3 & q_2 \\ q_2 & q_3 & q_0 & -q_1 \\ q_3 & -q_2 & q_1 & q_0 \end{pmatrix}$, $\boldsymbol{\Omega} = \begin{pmatrix} 0 \\ \omega_x^b \\ \omega_y^b \\ \omega_z^b \end{pmatrix}$.

In the body-fixed frame of a particle, the dynamic equations are [45]

$$\dot{\omega}_x^b = \frac{\tau_x^b}{I_{xx}} + \left(\frac{I_{yy} - I_{zz}}{I_{xx}}\right)\omega_y^b \omega_z^b$$

$$\dot{\omega}_y^b = \frac{\tau_y^b}{I_{yy}} + \left(\frac{I_{zz} - I_{xx}}{I_{yy}} \right) \omega_z^b \omega_x^b$$
$$\dot{\omega}_z^b = \frac{\tau_z^b}{I_{zz}} + \left(\frac{I_{xx} - I_{yy}}{I_{zz}} \right) \omega_x^b \omega_y^b \qquad (2)$$

Where τ_x^b, τ_y^b and τ_z^b are components of torque $\boldsymbol{\tau^b}$ expressed in body-fixed frame, ω_x^b, ω_y^b and ω_z^b are components of angular velocities measured in body-fixed frame, and I_{xx}, I_{yy} and I_{zz} are the three principle moments of inertia in body-fixed frame in which the inertia tensor is diagonal. In case of 3-D spheres, $I = I_{xx} = I_{yy} = I_{zz}$.

At each time step Eqs. 1-2 are integrated such that unique orientation of each particle is known at each time step. Details of the algorithm to solve Eqs. 1-2 can be found in (Wang et al 2006).

2.2 Full set of interactions

The second important difference is that a full set of interactions are included. There are three kinds of interactions in ESyS_Particle: bonded interaction, solely normal repulsive interaction and cohesionless frictional interaction (Wang et al, 2008). A special emphasis is placed on the bonded interaction in which all three interactions (normal, shearing forces and bending moment) are transmitted in 2-D and six (normal, shearing forces, bending and twisting moment) in 3-D (Fig. 1) are transmitted between each bonded particle pair.

2.3 New way of updating forces and torques

The third innovation is the way how forces and torques caused by the relative movements between two particles are updated. In other existing DEMs, the incremental method was used to update the interactions between particles. Instead of incremental method , ESyS_Particle uses Finite Deformation Method, in which the total relative (translational and rotational) displacements are calculated at each time step.

Using quaternion algebra, we proved that () an arbitrary rotation between two rigid bodies or two coordinate systems cannot be decomposed into three order independent rotations around three orthogonal axes. However it can be decomposed into two rotations, which correspond to the relative twisting and bending between two bodies in our model. The two rotations are sequence-independent. The beauty of this sequence-independent decomposition is that it respects the physical law and it is guaranteed that forces and torques decided by such a two-step rotation are unique. Numerical results show that when dealing with finite rotations of particles, the incremental method is not as stable and accurate as the method used in our model (Wang, et al, 2008).

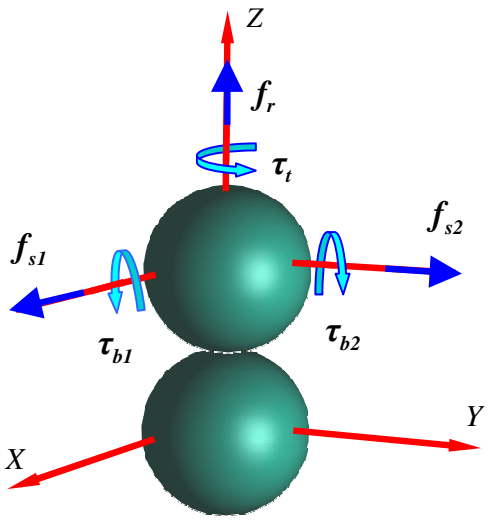

Figure 1 Six kinds of interactions between bonded particles. f_r is normal force, f_{s1} and f_{s2} are shear forces , τ_t is twisting torque, τ_{b1} and τ_{b2} are bending torque.

2.4 The criterion for bond breakage

In ESyS_Particle model, a bond breaks if the pure extensional force exceeds the threshold $f_r \geq F_{r0}$ (but it does not break under pure compression) , or the pure shear force $|f_s| \geq F_{s0}$, or the pure twisting torque $|\tau_t| \geq \Gamma_{t0}$, or the pure bending torque $|\tau_b| \geq \Gamma_{b0}$.

When all the interactions exist at the same time, the following empirical criterion is used to judge whether or not a bond is going to break

$$\frac{f_r}{F_{r0}} + \frac{|f_s|}{F_{s0}} + \frac{|\tau_t|}{\Gamma_{t0}} + \frac{|\tau_b|}{\Gamma_{b0}} \geq 1 \qquad (3)$$

We set f_r positive under extension and negative under compression such that it is more difficult for a bond to break under compression than under extension, and the effects of normal force on breakage of the bond has been taken into account.

2.5 Calibration of the model

We studied analytically how the particle scale stiffnesses are related to the macroscopic elastic constants of materials (). We found that the 2-D triangular lattice of equal-sized particles yields isotropic elasticity, and the normal, shear and bending stiffnesses are related to Young ‘s modulus *E* and passion ‘s ratio ν

$$K_r = \frac{\sqrt{3}E}{3(1-\nu)}, K_s = \frac{1-3\nu}{1+\nu}K_r, K_b = \frac{\sqrt{3}(1+\nu)(1-2\nu)ER^2}{36(1-\nu)} \qquad (4)$$

However, in 3-D case, the closest packing generates anisotropic elasticity, for example, Face-Centered Cubic (FCC) yields cubic elasticity, the simplest case for an orthotropic solid. The normal, shear, bending and twisting stiffnesses are decided using

$$K_r = \frac{\sqrt{2}ER}{2(1-2\nu)}\ , K_s = \frac{1-3\nu}{1+\nu}K_r\ ,$$

$$K_b = \frac{\sqrt{2}ER^3}{48(1-\nu)} = \frac{(1-2\nu)R^2}{24(1-\nu)}K_r\ ,\quad K_t = \frac{1-3\nu}{1+\nu}K_b = \frac{(1-2\nu)R^2}{24(1-\nu)}K_s \tag{5}$$

Where R is the radius of particles. If the particle stiffnesses are chosen according to Eq. (4)-(5), the realistic macroscopic elasticity is guaranteed.

The source code is written in C++ with a Python script interface. Physics parameters, integration steps, types of particles, types of loading walls, the contact properties, artificial viscosity, ways of loading and output fields are specified in the script. Pre-processing includes a particle generation package, and the post-processing includes Povray and VTK visualization packages. The code is parallelized using MPI.

3 Fracture patterns and size distribution

3.1 Algorithm to calculate fragment sizes

In ESyS_Particle, the breakage of bonds is explicit representation of fracture. Under loading some bonds break, but some are still intact. At certain time interval we output the bonding information. These include information of particle pairs which are still bonded. Then a special algorithm is developed to judge which particles belong to a group (fragment). The idea is that if two particles are bonded, they belong to the same fragment. if another particle is bonded to any of the particles in the group, it joins the group. This process repeats until a particle is not bonded to any of the particles in the existing groups, then it starts a new group. If two particles from two different fragments are found to be linked, the two fragments are combined into one. In this way all particles can be grouped to corresponding groups. By calculating the volume of each fragment, the size distribution plot can be obtained.

3.2 Mass distribution of fragments under slow uniaxial compression

Fig. 2 shows fractures pattern of a 3-D brittle rock-like material at four different stages. In this example, the sample consisting of random sized particle bonded together is subjected to a slow uniaxial compression in the vertical direction. The colors represent vertical displacements. Discontinuities in colors mean the formation of fractures which is difficult to be captured in laboratory tests since this process always occurs very fast. When the main faults are formed, two intact cores can be clearly observed with small fragile parts shattering away. This kind of pattern is always observed in rock fracture tests.

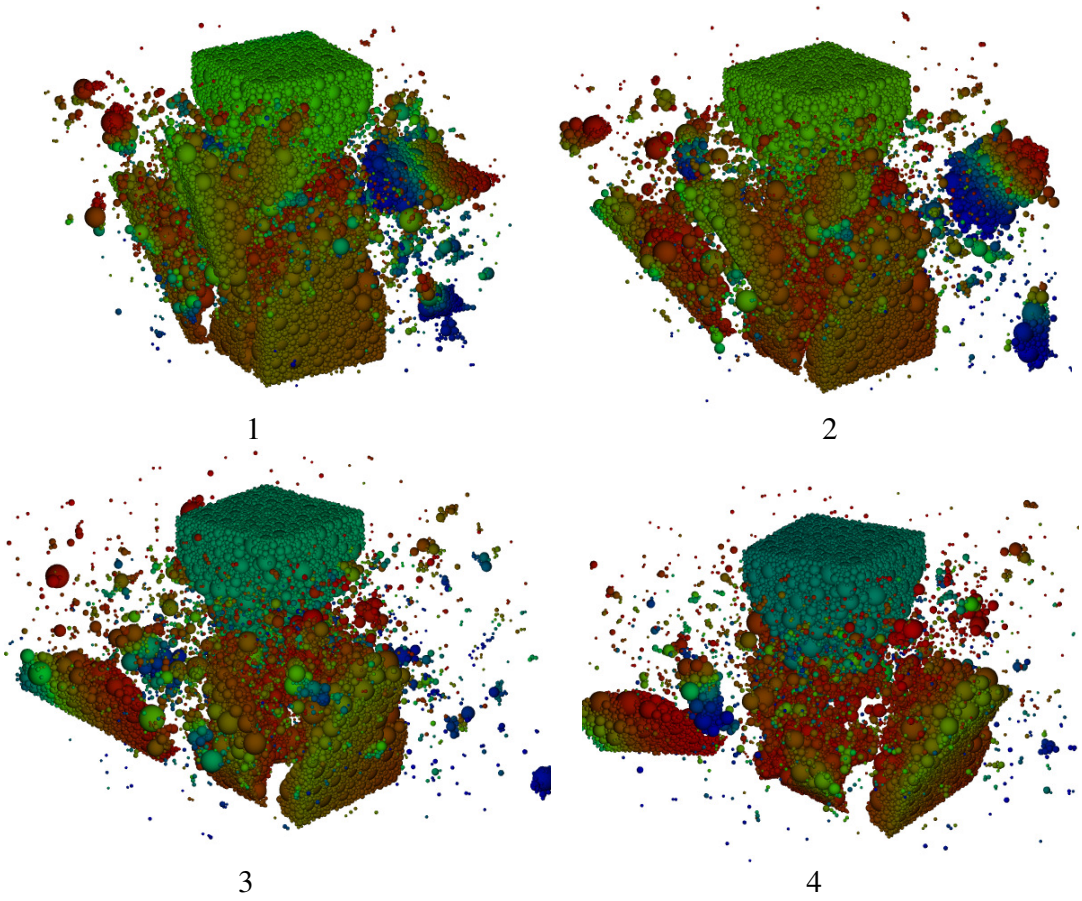

Fig. 2 Four stages of fragmentation under slow uni-axial compression.

Fig. 3 plots the size distribution of Fig. 2. It shows the relative percentage of different volume size, defined by the number of fragments with each volume size divided by the total number of fragments. Except for the largest fragment sizes, a power law distribution with an exponent τ=-0.75 are observed for nearly four orders of magnitude in volume. It is also noticed that with time increase, the relative percentages drop at volume between 0.1 to 10. This can be explained by continuing fracture during this time.

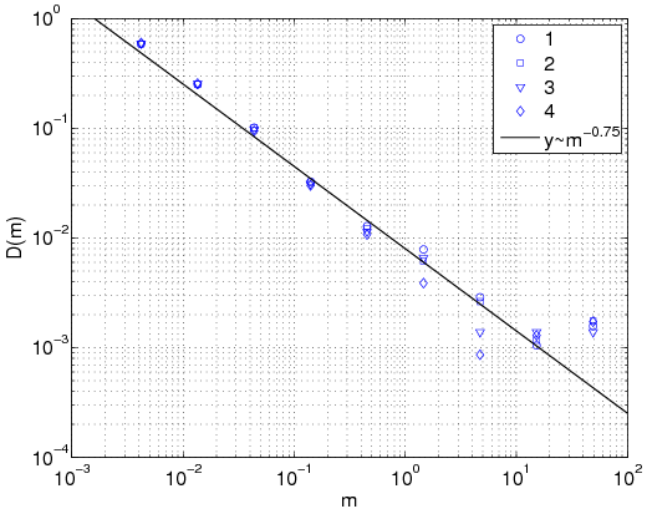

Fig. 3 Fragmentation size distribution of Fig. 2. Number 1-4 represent the four stages. The volume of the fragment is represented by m.

3.3 Size distribution under fast loading : impact fracture of a ball to a rigid wall

Fig. 4 shows three snapshots of fracture patterns of a ball after impacting to a rigid wall at different velocities. When the velocity is small (v = 4Vo), only slight damage can be observed, and the ball mainly keeps its integrity increasing the velocity, the specimen breaks into more pieces, in a good agreement with the laboratory tests (Wu et al 2004) and numerical simulations (Thornton et al 2004). The fragmentation size distribution can be found in Fig. 5. Up to the size of 0.1 power laws with the same exponent τ=-0.75 are observed for all the three velocities. Large deviations from the linear lines are observed for large fragment volumes. Generally it is observed that higher velocity means more fragments. It is interesting to note in Fig. 5 that in case of higher velocity the largest piece generated is smaller than that of small velocity, indicating the important role of input energy.

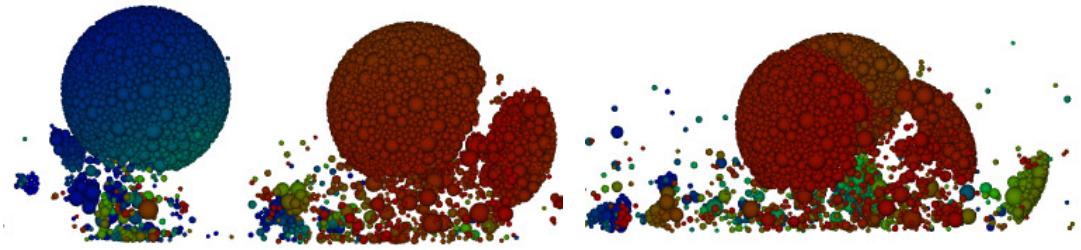

Fig. 4 Fracture patterns of a ball impacting to a rigid wall at different impact velocities.

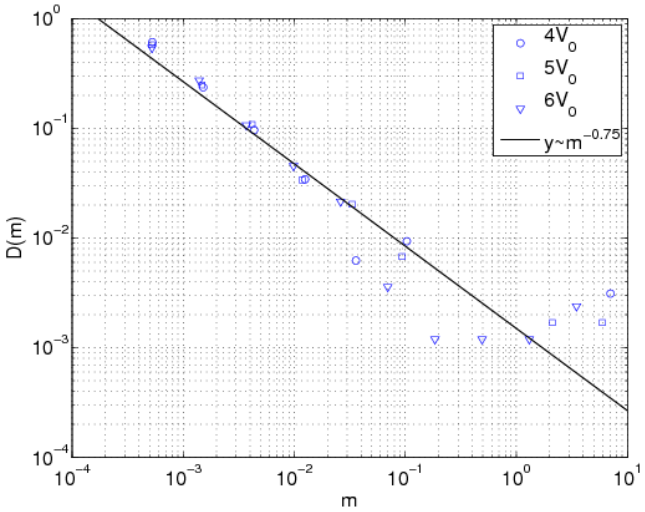

Fig. 5 Fragmentation size distribution for three different impacting velocities.

4 Summary and discussions

In this short paper, we briefly introduced our Discrete Element Model, ESyS_Particle. The most important features which distinguish ESyS_Particle from the other existing DEMs are: explicit representing of particle orientation using unit quaternion, complete interactions (six kinds of independent relative movements are transmitted between two 3-D interacting particles) and the new way of decomposing the relative rotations between two rigid bodies in such a way that the torques and forces caused by such relative rotations can be uniquely determined.

Using this model, we studied brittle fracture of rock-like materials under two types of loading conditions: the fracture of a square-shaped rock under slow uniaxial compression and dynamic fracture of a sphere colliding to a rigid wall. The basic features of fragmentation patterns are well reproduced.

An algorithm was developed to calculate the size of fragments. Except for the largest fragments, we obtained power law size distribution for nearly four orders of magnitude in volume, independent of the specimen shapes and loading conditions. The origin of the power laws distributions of size is still not clear. Previous studies based on percolation clusters of broken bonds were successful to explain the power laws, but they failed in the prediction of the exponents (Kun et al 1999).

The larger deviations for large fragments were also reported by other studies (Wu et al 2004). Some even suggest that coarse and fine fragments obey to two different power law distributions (Wu et al 2004). Based on numerical experiments (Thornton et al 2004) it is suggested that the coarser fragments result from cracks propagated from the loading/impact zone, whereas the finer fragments result from secondary fragments created perpendicular to the fractured surfaces. The question is: Is the deviations for large fragments caused partly by the size effects, or it is underlain by different physical mechanisms? The studies in this paper are still rudimentary. More large scale simulations are required to investigate these problems in the future.

Acknowledgements

We thank for the support of the ACcESS and AuScope project, and the Australian Research Council (project number DP0772409).

References

Thornton, C. and Ciomocos, MT and Adams, MJ, Numerical simulations of diametrical compression tests on agglomerates, Powder Technology,140, 258-267,2004

Kanchibotl, SS, Optimum blasting? Is it minimum cost per broken rock or maximum value per broken rock? Fragblast(Rotterdam), 7, 35-48, 2003.

Wu, SZ and Chau, KT and Yu, TX, Crushing and fragmentation of brittle spheres under double impact test, Powder Technology, 143, 41-55, 2004

Kun, F. and Herrmann, H.J., Transition from damage to fragmentation in collision of solids, Physical Review E, 59, 2623—2632, 1999

Wang Y.C, S. Abe, S. Latham and P. Mora, *Implementation of particle-scale rotation in the 3D*, Pure Appl. Geophys. 1769-1785, (2006).

Wittel, F. and Kun, F. and Herrmann, HJ and Kroplin, BH, Fragmentation of Shells, Physical Review Letters, 93, 355504, 2004.

Wilson, B. and Dewers, T. and Reches, Z. and Brune, J, Particle size and energetics of gouge from earthquake rupture zones, Nature, 434, 749-52, 2005